

See discussions, stats, and author profiles for this publication at: <https://www.researchgate.net/publication/260808428>

# S-P Coupling Induced Unusual Open-shell Metal Clusters.

ARTICLE in JOURNAL OF THE AMERICAN CHEMICAL SOCIETY · MARCH 2014

Impact Factor: 12.11 · DOI: 10.1021/ja412637j · Source: PubMed

CITATIONS

5

READS

28

## 4 AUTHORS, INCLUDING:



**Shibo Cheng**

Pennsylvania State University

19 PUBLICATIONS 75 CITATIONS

SEE PROFILE



**Cunevt Berkdemir**

Pennsylvania State University

47 PUBLICATIONS 794 CITATIONS

SEE PROFILE



**Joshua Melko**

University of North Florida

38 PUBLICATIONS 188 CITATIONS

SEE PROFILE

## S-P Coupling Induced Unusual Open-Shell Metal Clusters

Shi-Bo Cheng,<sup>†</sup> Cuneyt Berkdemir,<sup>†,‡</sup> Joshua J. Melko,<sup>†,§</sup> and A. W. Castleman, Jr.\*<sup>†,‡</sup><sup>†</sup>Department of Chemistry and <sup>‡</sup>Department of Physics, The Pennsylvania State University, University Park, Pennsylvania 16802, United States

## S Supporting Information

**ABSTRACT:** Metal clusters featuring closed supershells or aromatic character usually exhibit remarkably enhanced stability in their cluster series. However, not all stable clusters are subject to these fundamental constraints. Here, by employing photoelectron imaging spectroscopy and ab initio calculations, we present experimental and theoretical evidence on the existence of unexpectedly stable open-shell clusters, which are more stable than their closed-shell and aromatic counterparts. The stabilization of these open-shell Al-Mg clusters is proposed to originate from the S-P molecular orbital coupling, leading to highly stable species with increased HOMO–LUMO gaps, akin to s-p hybridization in an organic carbon atom that is beneficial to form stable species. Introduction of the coupling effect highlighted here not only shows the limitations of the conventional closed-shell model and aromaticity but also provides the possibility to design valuable building blocks.

Searching for stable clusters, which can be used as building blocks in the application of cluster-assembled nanomaterials,<sup>1a,b</sup> has become one of the main subjects in cluster science.<sup>1c–f</sup> An equally important task is to explore simple models to understand the origin of their enhanced stability. In cluster science, there are several electron counting rules or models that have been utilized effectively to design stable metal clusters and synthesize cluster-assembled materials.<sup>2</sup> Among the various models, the electronic closed-shell model is perhaps the most widely used tool to account for the special stability of metal clusters.<sup>3</sup> In this model, valence electrons from individual atoms in the cluster exist in a uniform background potential, and clusters containing a magic number of electrons (2, 8, 18, 20, ...) will have closed shells and enhanced stability. The “magic” Al<sub>13</sub><sup>−</sup> cluster is a popular example, which has 40 valence electrons.<sup>4</sup> Another well-known model is aromaticity, which has historically been applied to organic systems that are planar, cyclic, and stabilized by (4*n* + 2)  $\pi$  electrons. Only recently has this concept been extended by Li et al. to all-metal systems, which makes this boundary between organic and inorganic chemistry flexible.<sup>5</sup> Subsequently, the concept of all-metal aromaticity has been employed in many studies to account for the enhanced stability of magic metal clusters.<sup>6</sup> While these models have been useful in explaining cluster stabilities, one may ask whether there is a possibility of synthesizing a cluster that is more stable than its closed-shell and aromatic analogues. Additionally, s-p hybridization is a fundamental concept in organic chemistry, where the s- and p-orbitals are mixed to form hybridized orbitals beneficial to producing stable species.

May a similar concept occur in the molecular orbitals of clusters to stabilize inorganic metal clusters?

We explored these questions by investigating the electronic structures of small Al-Mg clusters through a synergistic approach combining velocity map imaging (VMI) and ab initio calculations. Photoelectron spectroscopy (PES), especially the VMI technique, combined with high-level theoretical calculations has been demonstrated to be a powerful tool for directly probing the electronic properties of clusters.<sup>7</sup> Herein, we present experimental and theoretical evidence on the existence of unexpectedly triplet ground states of two small Al-Mg clusters, namely AlMg<sub>2</sub><sup>−</sup> and Al<sub>2</sub>Mg. Particularly, <sup>3</sup>AlMg<sub>2</sub><sup>−</sup> is more stable than its closed-shell and aromatic <sup>1</sup>AlMg<sub>2</sub><sup>−</sup> counterpart, showing the limitations of the conventional electronic closed-shell model and aromaticity. The stabilization of these open-shell Al-Mg clusters is proposed to originate from the S-P molecular orbital coupling (the uppercase S and P refer to molecular orbitals, while the lowercase s and p refer to atomic orbitals throughout the whole paper), leading to highly stable species with increased HOMO–LUMO gaps, akin to s-p hybridization in the organic carbon atom. The introduction of the coupling effect highlighted here not only extends the fundamental function of hybridization to all-metal clusters but also may stimulate further efforts in designing valuable building blocks.

A typical mass spectrum (Figure 1) of small Al<sub>*n*</sub>Mg<sub>*m*</sub><sup>−</sup> clusters synthesized in our cluster source (see the Supporting Information) shows that, in the case of the Al<sub>*n*</sub>Mg<sub>*m*</sub><sup>−</sup> cluster series, AlMg<sub>2</sub><sup>−</sup> stands out as the more abundant species, indicating an enhanced stability which is discussed below. The

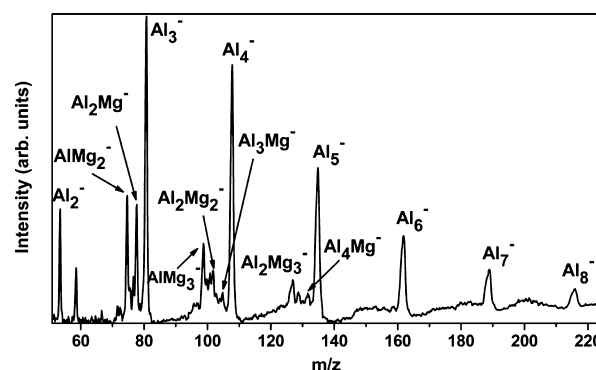
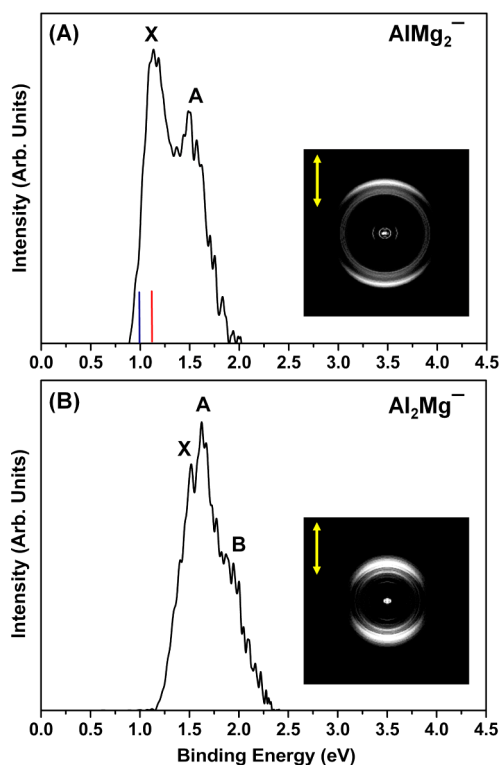


Figure 1. Collected mass spectrum of small Al-Mg cluster anions.

Received: December 23, 2013

Published: March 13, 2014

VMI experiments were focused on the two most intense  $\text{Al}_n\text{Mg}_m^-$  peaks, which are  $\text{AlMg}_2^-$  and  $\text{Al}_2\text{Mg}^-$ . The photoelectron images and corresponding photoelectron spectra (Figure 2) were obtained at 532 nm. Two prominent peaks



**Figure 2.** Photoelectron images and corresponding photoelectron spectra for (A)  $\text{AlMg}_2^-$  and (B)  $\text{Al}_2\text{Mg}^-$  obtained at 532 nm. Laser polarization is vertical in the plane of the page.

(X and A) were observed in the spectrum of  $\text{AlMg}_2^-$  (Figure 2A). The photoelectron angular distribution (PAD) of band X is preferably oriented parallel to the laser polarization, and the measured anisotropy parameter ( $\beta$ ) is 0.9, indicating that the detachment process likely occurs from a molecular orbital (MO) composed mainly of the  $\sigma$ -type orbital.<sup>8</sup> In the case of  $\text{Al}_2\text{Mg}^-$  (Figure 2B), three primary transitions, designated X, A, and B, were detected, in which feature B is a shoulder to A. The experimentally measured adiabatic detachment energies (ADEs), vertical detachment energies (VDEs), and  $\beta$  values (see Table S1 in the Supporting Information) are compared to the results of *ab initio* calculations discussed below.

We performed electronic structure calculations (see the Supporting Information) to search for the lowest energy structures (Figure S1) of the small Al-Mg clusters, in order to draw a clearer picture of the structural and electronic properties and the relative stability. The Al–Mg bond length in neutral  $\text{AlMg}$  is calculated to be 2.930 Å, which is in excellent agreement with the recently reported value of 2.94 Å.<sup>9</sup> Additionally, the PES bands (Figure 2) serve as an electronic fingerprint for the clusters, allowing comparison with theoretical ADEs and VDEs to validate optimized structures. Good agreement is seen between experimental and theoretical ADEs and VDEs of  $\text{AlMg}_2^-$  and  $\text{Al}_2\text{Mg}^-$  (see Table S1 in the Supporting Information), providing confidence in our calculated ground-state structures and spin multiplicities.

Our mass distribution (Figure 1) shows an enhanced stability of  $\text{AlMg}_2^-$ , as mentioned earlier. To gain insights into the magic numbers of the small Al-Mg clusters, we now turn our attention to their relative stability. One criterion to explore is the energy gap between the highest occupied molecular orbital (HOMO) and the lowest unoccupied molecular orbital (LUMO), termed the H-L gap. A large gap is a signature of enhanced stability and reduced reactivity.<sup>10</sup> Calculated H-L gaps (see Figure S2A in the Supporting Information) are plotted versus number of valence electrons. As suggested in previous studies,<sup>9,11</sup> we determined the number of valence electrons,  $N(e^-)$ , by simply counting Al and Mg atoms as having three and two valence electrons, respectively. Among the neutral series,  $\text{Al}_2\text{Mg}$  has the largest H-L gap of 1.68 eV, which is close to the values of the  $\text{C}_{60}$  cluster (1.70 eV)<sup>12</sup> and the superatomic species  $\text{Al}_{13}^-$  (1.87 eV).<sup>1e,13</sup> As for the anions, the largest H-L gap belongs to  $\text{AlMg}_2^-$ , indicating an enhanced stability, which is consistent with our mass distribution. As a further probe of the relative stability, we calculated the fragmentation behavior of these Al-Mg clusters, providing the thermodynamic stability (Figure S2B). The  $\text{AlMg}_2^-$  and  $\text{Al}_2\text{Mg}$  clusters have the largest fragmentation energies in their respective cluster series, which are 0.80 and 0.93 eV, indicating the enhanced stability.

It is evident that, in both cluster series, the chemical and energetic stability of the clusters is maximized at 8  $e^-$ , which is a magic number in the electronic closed-shell framework.<sup>3b,14</sup> Moreover,  $\text{Al}_5\text{Mg}_2^-$  and  $\text{Al}_{11}\text{Mg}_3^-$  have 20 and 40  $e^-$ , respectively, and they have been found to exhibit enhanced stability, which can be rationalized within an electronic closed-shell model.<sup>11</sup> These findings make us suspect that the model may be applied again to these smaller triatomic systems. It is surprising, however, that the experimentally and theoretically verified ground-state structures of  $\text{AlMg}_2^-$  and  $\text{Al}_2\text{Mg}$  have unexpectedly triplet multiplicities, implying the electronic shells are not closed, inconsistent with the shell-closing model. To further verify that the ground state of  $\text{AlMg}_2^-$  is triplet, the VDE of the singlet  $\text{AlMg}_2^-$  was also calculated, marked as a blue line in Figure 2A, while that of  $^3\text{AlMg}_2^-$  is marked as a red line for comparison. The result from  $^3\text{AlMg}_2^-$  matches the experimental data better than that from  $^1\text{AlMg}_2^-$ .

Thus, interesting questions arise: what is the energy splitting ( $\Delta E_{\text{st}}$ ) between  $^1\text{AlMg}_2^-$  and  $^3\text{AlMg}_2^-$ , and does metastable  $^1\text{AlMg}_2^-$  follow the electronic closed-shell configuration? We answer these questions by calculating the one-electron energy levels and the associated electronic orbitals of  $\text{AlMg}_2^-$  (Figure 3A,B). Based on the present theoretical level,  $^1\text{AlMg}_2^-$  is 0.11 eV higher in energy than  $^3\text{AlMg}_2^-$ . The HOMO (Figure 3B) of  $^3\text{AlMg}_2^-$  is a  $\sigma$ -type MO, implying that it is the  $\sigma$ -type orbital from which detachment occurred in  $^3\text{AlMg}_2^-$ , leading to  $^2\text{AlMg}_2$ . This is consistent with our experimentally measured PAD and  $\beta$  value mentioned earlier. In contrast, the HOMO of  $^1\text{AlMg}_2^-$  (Figure 3A) is a delocalized  $\pi$ -type orbital, which is not supported by our experiments. Such a result gives further evidence that the ground state of  $\text{AlMg}_2^-$  is triplet. Prior to investigating the origin of enhanced stability in  $^3\text{AlMg}_2^-$ , we focus on the electronic properties of  $^1\text{AlMg}_2^-$ . In  $^1\text{AlMg}_2^-$ , all eight valence electrons are filled in the highest four occupied orbitals. Starting around  $-0.20$  eV is a delocalized orbital well spread over the cluster, which could be regarded as a 1S orbital in closed-shell framework. Following this, three orbitals representing  $p$ -type states can be marked as the  $P_x$ ,  $P_y$ , and  $P_z$  orbitals. Above these are the unfilled MOs: the first unfilled one

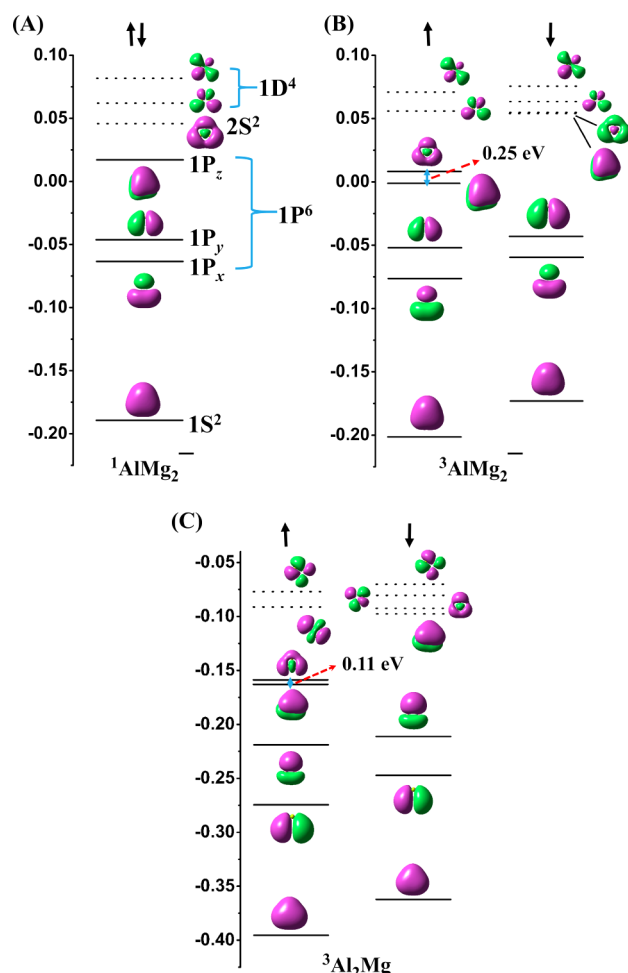


**Figure 3.** One-electron energy levels and orbital isosurfaces (isoval = 0.01 au) for the (A)  $^1\text{AlMg}_2^-$ , (B)  $^3\text{AlMg}_2^-$ , and (C)  $^3\text{Al}_2\text{Mg}$  clusters. The continuous lines correspond to the occupied states, and the dashed lines represent unoccupied levels. The up and down arrows indicate the majority (up) and minority (down) spin states, respectively. Energy is in units of eV.

is nearly symmetric and could be labeled as a 2S shell, followed by the 1D-type orbitals.<sup>15</sup> The orbital shapes of  $^1\text{AlMg}_2^-$  nicely match the electronic closed-shell configuration. So the  $^1\text{AlMg}_2^-$  can be considered as an electronic closed-shell species.

Moreover, as evidenced in Figure 3A, the HOMO of  $^1\text{AlMg}_2^-$  is a typically delocalized  $\pi$  orbital with two electrons, satisfying the  $(4n + 2) \pi$  electron Hückel rule for aromaticity. To further verify whether the aromatic concept is applicable, we calculated the nucleus-independent chemical shift (NICS) (see Table S2 in the Supporting Information), which is one of the most popular approaches for diagnosing aromaticity, proposed by Schleyer et al.<sup>16</sup> Systems with negative NICS are aromatic, while those with positive NICS are antiaromatic. The negative NICS values are evidence for the aromaticity of  $^1\text{AlMg}_2^-$ . In addition to NICS values, the magnetic susceptibility anisotropy  $\Delta\chi$  is often used as a probe of aromaticity.<sup>17</sup> Similar to NICS, aromatic clusters possess negative  $\Delta\chi$ . The theoretical  $\Delta\chi$  value for  $^1\text{AlMg}_2^-$  is  $-91.0$  cgs-ppm calculated at the B3LYP/6-311++G(3df,3pd) level of theory, which further confirms its aromatic character. Therefore,  $^1\text{AlMg}_2^-$  seems to satisfy both the electronic closed-shell model and all-metal aromaticity, implying that it could be expected to be very stable.

Surprisingly, such a closed-shell and aromatic species  $^1\text{AlMg}_2^-$  is not the ground state of  $\text{AlMg}_2^-$ . So what governs the unexpected stability of the open-shell  $^3\text{AlMg}_2^-$ ? Comparing the MOs of  $^1\text{AlMg}_2^-$  and  $^3\text{AlMg}_2^-$  (Figure 3A,B), one  $1P_z$  (minority) orbital in  $^3\text{AlMg}_2^-$  is pushed up in energy, becoming the LUMO, and simultaneously one 2S (majority) orbital is stabilized as the HOMO, substantially increasing the H-L gap to form a stable open-shell cluster. Interestingly, the spacing between the HOMO (S-like) and HOMO-1 (P-like) MOs in  $^3\text{AlMg}_2^-$  is very small (0.25 eV), which may induce coupling between them, analogous, although not exactly identical, to the s-p hybridization in organic carbon chemistry, followed by the splitting of the HOMO and LUMO orbitals.

The s-p hybridization of orbitals in organic carbon chemistry is greatly favored in that hybridized orbitals could form more bonds than their unhybridized and separated counterparts, which is beneficial to form more stable compounds. Similarly, the S-P molecular orbital coupling observed here efficiently stabilizes the orbital energy (Figure 3B), leading to a more stable open-shell triplet cluster with increased H-L gap. The credence for the existence of such S-P coupling can be further probed by examining the MOs of  $^3\text{Al}_2\text{Mg}$  (Figure 3C). In  $\text{Al}_2\text{Mg}$ , the calculated energy splitting between singlet and triplet states is even larger (0.21 eV). As expected, the S-P coupling is stronger in  $^3\text{Al}_2\text{Mg}$ , as evidenced by the smaller spacing between H and H-1 orbitals (0.11 eV, Figure 3C), which also corresponds to a larger H-L gap (1.68 eV). Therefore, it demonstrates that stronger S-P coupling better stabilizes the triplet state of the cluster and induces enhanced stability (larger H-L gap). To shed light on this suggestion, we calculated the S-P coupling dependence of the H-L gap (Figure 4) in  $^3\text{AlMg}_2^-$ . By gradually decreasing the spacing between the

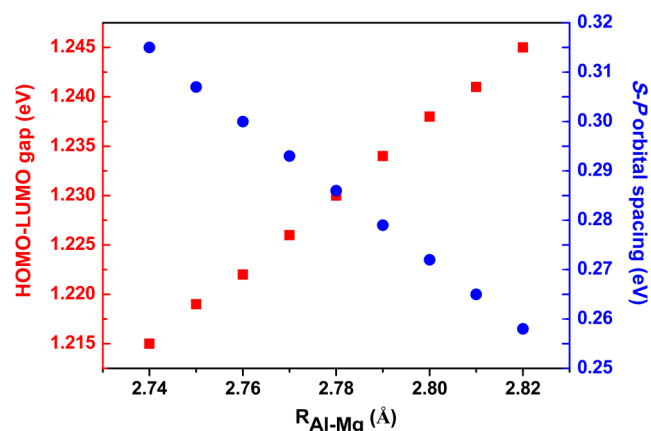


**Figure 4.** S-P coupling (blue circle) dependence of the H-L gap (red square) in  $^3\text{AlMg}_2^-$ . Energy is in units of eV.

S- and P-like orbitals (stronger S-P coupling), achieved by changing the Al-Mg bond length in  $^3\text{AlMg}_2^-$ , we observed larger H-L gaps. Thus, there exists significant correlation between these two variables, supporting our proposed mechanism.

It is necessary to note that the ground states of metal clusters that possess triplet or higher spin multiplicity are not a surprise to the chemistry community.<sup>18</sup> However, the most important finding in the present study is that the singlet  $\text{AlMg}_2^-$ , satisfying both the electronic closed-shell model and all-metal aromaticity, is not the most stable electronic configuration of  $\text{AlMg}_2^-$ ,



which is unusual based on the well-accepted closed-shell and aromaticity models. The novel finding highlighted here is that the most stable electronic state of  $\text{AlMg}_2^-$  is not only triplet but also more stable than its closed-shell and aromatic counterpart  $^1\text{AlMg}_2^-$ . Additionally, since the S-P coupling effect has been evidenced to account for the enhanced stability of the open-shell triplet Al-Mg clusters as discussed above, it would be beneficial if we could determine the magnitude of this coupling effect quantitatively, which is beyond the scope of this Communication and our ability. Therefore, novel and higher-level theoretical methods considering electron correlation and multireference character are urgently desired to quantitatively describe such an important coupling effect.

In summary, the current investigation presents evidence on the existence of unexpectedly stable open-shell Al-Mg clusters. The  $^3\text{AlMg}_2^-$  cluster is found to be more stable than its closed-shell and aromatic  $^1\text{AlMg}_2^-$  counterpart. A new model, namely S-P molecular orbital coupling, is observed to play an important role in stabilizing the open-shell clusters, analogous to the s-p hybridization in organic carbon chemistry. The enhanced stability of the open-shell clusters observed here shows the limitations of the conventional electronic closed-shell model and aromaticity. We believe that the introduction of S-P coupling in metal clusters highlighted here will stimulate further efforts to explore new mechanisms governing cluster stability, which will be of value in designing valuable building blocks in the application of cluster-assembled nanomaterials. The present two cluster systems ( $^3\text{AlMg}_2^-$  and  $^3\text{Al}_2\text{Mg}$ ) offer the first example of this novel coupling effect. In addition, other clusters featuring the same coupling effect have already been found in our group, and will be discussed in another individual work. This convinces us that such a coupling effect may broadly exist in metal clusters. Moreover, due to the involvement of d or f electrons in heavier metal elements, similar coupling effects (P-D or D-F type coupling) may also exist in heavier metal clusters, which could produce stable open-shell species of larger sizes.

## ■ ASSOCIATED CONTENT

### Supporting Information

Text, tables, and figures giving further experimental and theoretical details. This material is available free of charge via the Internet at <http://pubs.acs.org>.

## ■ AUTHOR INFORMATION

### Corresponding Author

awc@psu.edu

### Present Addresses

<sup>§</sup>J.J.M.: Air Force Research Laboratory, Space Vehicles Directorate, Kirtland AFB, NM 87117-5776

<sup>#</sup>C.B.: Department of Physics, Yildiz Technical University, Istanbul, 34210, Turkey

### Notes

The authors declare no competing financial interest.

## ■ ACKNOWLEDGMENTS

This material is based upon work supported by the Air Force Office of Science Research under AFOSR Award No. FA9550-10-1-0071.

## ■ REFERENCES

- (1) (a) Khanna, S. N.; Jena, P. *Phys. Rev. Lett.* **1992**, *69*, 1664. (b) Khanna, S. N.; Jena, P. *Phys. Rev. B* **1995**, *51*, 13705. (c) Li, X.; Grubisic, A.; Stokes, S. T.; Cordes, J.; Gantefer, G. F.; Bowen, K. H.; Kiran, B.; Willis, M.; Jena, P.; Burgert, R.; Schnoeckel, H. *Science* **2007**, *315*, 356. (d) Bergeron, D. E.; Roach, P. J.; Castleman, A. W., Jr.; Jones, N. O.; Khanna, S. N. *Science* **2005**, *307*, 231. (e) Bergeron, D. E.; Castleman, A. W., Jr.; Morisato, T.; Khanna, S. N. *Science* **2004**, *304*, 84. (f) Ugrinov, A.; Sen, A.; Reber, A. C.; Qian, M.; Khanna, S. N. *J. Am. Chem. Soc.* **2008**, *130*, 782.
- (2) Jena, P. *J. Phys. Chem. Lett.* **2013**, *4*, 1432.
- (3) (a) de Heer, W. A. *Rev. Mod. Phys.* **1993**, *65*, 611. (b) Knight, W. D.; Clemenger, K.; de Heer, W. A.; Saunders, W. A.; Chou, M. Y.; Cohen, M. L. *Phys. Rev. Lett.* **1984**, *52*, 2141.
- (4) Leuchtner, R. E.; Harms, A. C.; Castleman, A. W., Jr. *J. Chem. Phys.* **1989**, *91*, 2753.
- (5) Li, X.; Kuznetsov, A. E.; Zhang, H. F.; Boldyrev, A. I.; Wang, L. S. *Science* **2001**, *291*, 859.
- (6) Boldyrev, A. I.; Wang, L. S. *Chem. Rev.* **2005**, *105*, 3716.
- (7) (a) Yandell, M. A.; King, S. B.; Neumark, D. M. *J. Am. Chem. Soc.* **2013**, *135*, 2128. (b) Zhang, X.; Wang, Y.; Wang, H.; Lim, A.; Gantefer, G.; Bowen, K. H.; Reveles, J. U.; Khanna, S. N. *J. Am. Chem. Soc.* **2013**, *135*, 4856. (c) Li, R. Z.; Liu, C. W.; Gao, Y. Q.; Jiang, H.; Xu, H. G.; Zheng, W. J. *J. Am. Chem. Soc.* **2013**, *135*, 5190. (d) Bao, X.; Hrovat, D. A.; Borden, W. T.; Wang, X. B. *J. Am. Chem. Soc.* **2013**, *135*, 4291. (e) Sanov, A.; Lineberger, W. C. *Phys. Chem. Chem. Phys.* **2004**, *6*, 2018. (f) Verlet, J. R. R.; Bragg, A. E.; Kammrath, A.; Cheshnovsky, O.; Neumark, D. M. *Science* **2005**, *307*, 93. (g) Wenthold, P. G.; Lineberger, W. C. *Acc. Chem. Res.* **1999**, *32*, 597. (h) Cheng, S.; Berkdemir, C.; Melko, J. J.; Castleman, A. W., Jr. *J. Phys. Chem. A* **2013**, *117*, 11896. (i) Melko, J. J.; Werner, U.; Mitrić, R.; Bonačić-Koutecký, V.; Castleman, A. W., Jr. *J. Phys. Chem. A* **2011**, *115*, 10276. (j) Cheng, S. B.; Berkdemir, C.; Castleman, A. W., Jr. *Phys. Chem. Chem. Phys.* **2014**, *16*, 533.
- (8) Peppernick, S. J.; Gunaratne, K. D. D.; Castleman, A. W., Jr. *Proc. Natl. Acad. Sci. U.S.A.* **2010**, *107*, 975.
- (9) Osorio, E.; Vasquez, A.; Florez, E.; Mondragon, F.; Donald, K. J.; Tiznado, W. *Phys. Chem. Chem. Phys.* **2013**, *15*, 2222.
- (10) Reber, A. C.; Khanna, S. N.; Roach, P. J.; Woodward, W. H.; Castleman, A. W., Jr. *J. Am. Chem. Soc.* **2007**, *129*, 16098.
- (11) Luo, Z.; Grover, C. J.; Reber, A. C.; Khanna, S. N.; Castleman, A. W., Jr. *J. Am. Chem. Soc.* **2013**, *135*, 4307.
- (12) Wang, Y.; Holden, J. M.; Rao, A. M.; Lee, W. T.; Bi, X. X.; Ren, S. L.; Lehman, G. W.; Hager, G. T.; Eklund, P. C. *Phys. Rev. B* **1992**, *45*, 14396.
- (13) Khanna, S. N.; Rao, B. K.; Jena, P. *Phys. Rev. B* **2002**, *65*, 125105.
- (14) Janssens, E.; Tanaka, H.; Neukermans, S.; Silverans, R. E.; Lievens, P. *New J. Phys.* **2003**, *5*, 46.
- (15) Häkkinen, H. *Chem. Soc. Rev.* **2008**, *37*, 1847.
- (16) Schleyer, P. v. R.; Maerker, C.; Dransfeld, A.; Jiao, H. J.; Hommes, N. J. *J. Am. Chem. Soc.* **1996**, *118*, 6317.
- (17) Melko, J. J.; Ong, S. V.; Gupta, U.; Reveles, J. U.; D'Emidio, J.; Khanna, S. N.; Castleman, A. W., Jr. *Chem. Phys. Lett.* **2010**, *500*, 196.
- (18) (a) Cox, D. M.; Trevor, D. J.; Whetten, R. L.; Rohlfing, E. A.; Kaldor, A. *J. Chem. Phys.* **1986**, *84*, 4651. (b) Rao, B. K.; Jena, P. *J. Chem. Phys.* **1999**, *111*, 1890.